www.cadanda.com Computer-Aided Design and Applications

Computational Geometry Reconstruction from 3D Topology Optimization Results: A New Parametric Approach by the Medial Axis

Johannes Mayer[1] and Sandro Wartzack[2]

[1]Friedrich-Alexander-Universität Erlangen-Nürnberg, Engineering Design, Martensstraße 9, 91058 Erlangen, Germany, mayer@mfk.fau.de
[2]Friedrich-Alexander-Universität Erlangen-Nürnberg, Engineering Design, Martensstraße 9, 91058 Erlangen, Germany, wartzack@mfk.fau.de

Corresponding author: Johannes Mayer, mayer@mfk.fau.de

Abstract. Topology Optimization (TO) is used to develop high strength, yet lightweight structural components. The geometry reconstruction from raw optimization results is a crucial task and especially challenging to do considering product development's demand on parametrics. In this paper a new automated approach for computational reconstruction is presented that uses the Medial Axis for abstraction and inclusion of parametrics and features in the reconstruction. The presented method is both highly automated and at the same time offers optional geometry editing within the reconstruction itself. The steps of the method are (1) analysis of the TO result by the Voronoi computed Medial Axis Transform, (2) processing of the Medial Axis Transform into a decomposition, and (3) redesign thereon. Directly usable files of Computer-Aided Design (CAD) are generated. The concept is presented at real world case studies with focus on non-beam-like, structural components.

Keywords: Topology Optimization, Computer-Aided Design, Computational Design, Geometry Reconstruction, Skeletonization, Medial Axis Transformation.
DOI: https://doi.org/10.14733/cadaps.2023.960-975

1 INTRODUCTION TO TOPOLOGY OPTIMIZATION'S NEED FOR GEOMETRY RECONSTRUCTION

Lightweight design with high expectation on stiffness and strength as well as efficient use of material, is commonly pursued through Topology Optimization (TO) [6], [16], [32]. By this design method an optimized part topology can be determined from a given design space, loads and constraints. Among several other algorithms, the material distributing approach with Solid Isotropic Material with Penalization (SIMP) is widely spread due to its native connection to the commonly employed Finite Element Method (FEM) for structural analysis [6]. Given a volume fraction, the SIMP-method computes optimized material arrangement to meet the objective function, usually of minimal compliance.

Further constraints like active and passive voids, or simple manufacturing constraints can be considered. The outcome is a proposal of efficiently arranged material voxels in load path oriented layout. It is typically exported as a faceted (triangulated) geometry due to the underlying finite element mesh [35]. This generatively computed design proposal supports the development of stiff and strong lightweight products, enabling engineering structures of original shape and innovative designs. At the same time the development process itself is accelerated. Side by side to conventionally designing structures, the application of TO replaces time-consuming design cycles of trial and error by a requirement-oriented approach [16].

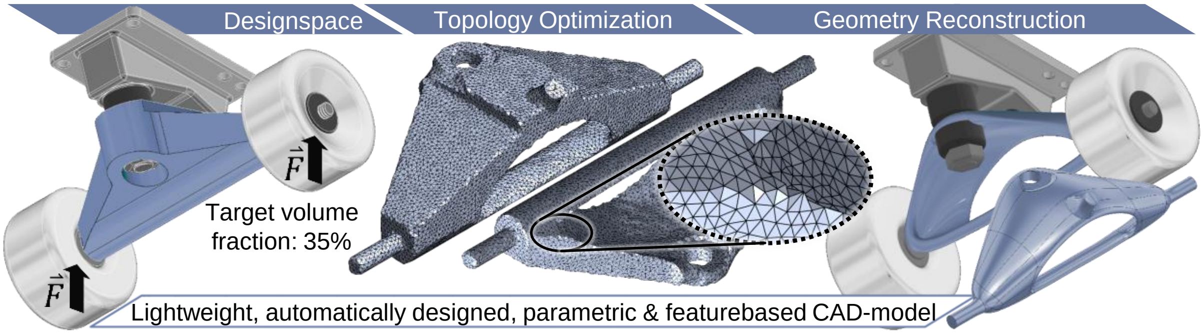

Figure 1: Exemplary application of topology optimization in product development of a sports device. The resulting CAD-file is generated with the presented approach.

For these reasons, TO has gained attention in design offices beyond being reserved to specialists [35]. Many products show successful lightweight design through TO, first in dedicated applications, but increasingly in more common products as well. Nevertheless, TO is still not as common as the reasons above suggest. A major hindering cause is the challenge of deriving the final product geometry from the unsteady boundary caused by the voxelized material-discretization-scheme [35]. Therefore, in most cases, a tedious *manual* redesign is required. Since the whole TO-procedure is geared towards the redesigned CAD-model, the reconstruction is a major [11], [35] or even the most important [16], [38], [40] part in the process. A survey amongst specialists of TO further exposes feature-based reconstruction of CAD-models as the main restrain (Fig. 2) [35].

Survey of users of Topology Optimization: What to include in Topology Optimization-Software?			
49 % Reconstruction of featurebased CAD-models	21 % Material anisotropy	17 % Other	13 % Multi-Mat.

Figure 2: Survey with responses of 85 users of topology optimization [35].

Beyond the remodeling of the design proposal itself, there are more efforts required to derive not a geometric model, but a feasible engineering solution: design rules and manufacturing constraints have to be considered according to the requirements. Reconstructed designs are largely dependent on engineering experience and expert knowledge and therefore hardly reproducible. The process is very time consuming. Lastly, manual reconstruction does not necessarily guarantee parametric changes, which are important for downstream applications of the product development process (PDP). The reconstructed model has to allow easy editability (e.g. thickness edit) [35].

Summed up the TO's embedding in the PDP can be time-reducing, but its lack of integration counteracts this benefit. While the workflow of computer-assistance up to the point, where TO is applied, is fluent, the manual reconstruction of a new CAD-Model is difficult and labor-intensive. Approaches to bridge this gap include solutions to merely smoothen the raw TO-result. This still does not yield an engineering solution and lacks usability, which is particularly necessary in the PDP. Research has developed approaches that don't require direct manual manipulation of the result, but perform a more automated reconstruction based upon a skeletal model instead. First approaches of this kind used lower dimensional 1D curve skeletons. These are unfortunately a special solution for the distinctive kind of beam-like TO-results and not applicable for general optimization results [3], [11], [34]. In contrast, an automated method producing feature-based, parametric models would be desirable. In consideration of the state of the art to curve skeletons in this field, the method should especially reconstruct non-beam-like structures. 3D surface skeletons seem to be better suited for more general and surface-like structures, but on the other hand are much harder to convert into an engineering solution [28]. Since they originate in the computer graphics field of expertise, they have to be adapted for the engineering driven purpose in geometry reconstruction. Both of these two disciplines are connected in our decomposition structure subsequent to the 3D surface skeleton. The term "decomposition structure" describes a set of purposefully processed information that enables geometry reconstruction.

For the research aim of converting TO's design proposal into a PDP-solution, this paper suggests a new skeleton-based approach. It is supposed to bridge the gap between TO and CAD-modeling with automated, computational design. It in deep focuses on how to adapt the skeletonization in an engineering context and convert the skeleton to a feasible CAD-model. This approach cuts the labor-intensive and time-consuming interpretation, and replaces it by a fast and assistive method with feasible results. Unlike previous approaches, the presented method is especially focused on non-beam-like optimized structures and on maintaining possibilities to edit the geometry even after the optimization run.

The paper is organized as follows. The next section (section 2) focuses on the previous work considering automated, parametric redesign. Emphasis lies on skeletonization-driven methods, since these focus on parametric and feature-based redesign. Section 3 introduces the Medial Axis Transform. Our approach is presented in section 4. Section 5 shows case studies of representative structures. After discussing the results in section 6, the paper ends with a conclusion on future research in this field of expertise in the final section 7.

2 RELATED WORK ON GEOMETRY RECONSTRUCTION FOR TOPOLOGY OPTIMIZATION

Computational approaches for geometry reconstruction can be categorized in volume-, surface- and skeleton-based strategies (Fig. 3) [35]. This depends in each case on whether volume decomposition takes place, the resulting surface is processed directly, or whether skeleton lines are extracted.

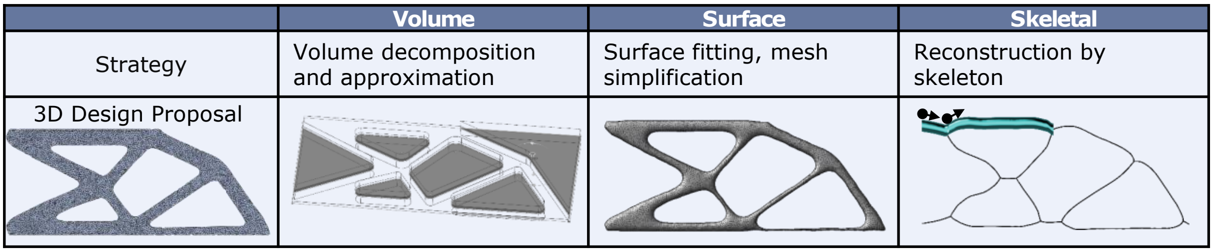

Figure 3: Classification of known geometry reconstruction methods [35].

Volume oriented: HSU M.-H. [18], HSU Y.-L. [19] and ZAHARINOV [42] use relevant cross-sections of the design proposal for an approximation with b-splines and connection through sweeping-operation to volume bodies. KALOUDIS and POULIAS [21] similarly use parametrized cross-sections of thin walled parts for manual placement upon the mesh. In a feature-based approach, LARSEN und JENSEN [24] present the usage of single, user picked areas of the design proposal in terms of pre-defined 2D cross-sections. These are subtracted from design space by Boolean operations. This subtractive strategy is bound to the main coordinate directions. These approaches face difficulties when subsequent cross-sections differ. For this reason, Subedi et al. [35] conclude, that volume orientied approaches are only feasible for sweeping-representable geometry. Automation herein is at least non-trivial due to the inevitably necessity of choosing relevant cross-sections and a sweeping-reference-curve.

Surface oriented: Surface oriented approaches for reconstruction of TO-results are most widely spread [35]. They principally either aim for remeshing the design proposal, subdividing the mesh or replacing the triangulation through parametric faces [35]. Kaloudis and Poulias [21] manually perform smoothing with optional patch segmentation and face generation upon single patches. Louhichi et al. [26] propose to split a previously subdivided design proposal in single, topologically logic surface-patches of polygonal format and specific boundary curve. From this, a B-Rep-model should be set together from parametric patches. Tang and Chang [38] approximate cross-sections by cubic b-splines and use them for the construction of a hull body in CAD. Koguchi and Kikuchi [22] classify each node of a design proposal as belonging to a corner, edge, or face, in order to keep corners and creases. Following to iso-faces computed by the marching-cubes-algorithm is an approximation of surface-patches with bi-quartic b-splines. In the same manner Hessel [17] performs a surface-segmentation and approximates the points through Non-Uniform-Rational-B-Splines (NURBS). A similar reconstruction strategy is shown by Joshi et al. [20]. Quadrangular polygons from voxelised data are used for C^1-smooth aggregation of NURBS-patches. Although TO is established part of numerous commercial software systems, most of these systems do not have an explicit geometry reconstruction. Most widely spread is the remodeling of the triangulated facets in surface-contour of the final model. In CAD-software PTC Creo Parametric the surface is smoothed by subdivision. [35] The software nTopology nTopPlatform uses an implicit representation of geometry and a smoothing of the design proposal [2]. In Robert McNeel & Associates Rhinoceros 3D, Altair solidThinking Inspire as well as 3D Systems Geomagic Design X and Autodesk Meshmixer, again NURBS are used for adaption of surface-patches to the triangulated data format. Autodesk Fusion 360 uses T-Splines for this [35]. Regardless the representation by triangulated data or NURBS-approximation, these models are represented by surfaces only. Therefore, parametric references and features are missing and so is practicable editing. The intention of product development with the possibility for design exploration (uncomplicated and fast performing controlled editing of a model) or the integration of manufacturing constraints aren't fulfilled this way. [35]

Skeleton oriented: To address this disadvantage, research has developed alternative approaches. They are based on skeletons as reference for parametric and feature-based geometry. In contrast to volume oriented strategies they do not work directly on the TO-result. Reconstruction strategies of this category all have the principle similarity to abstract the essential geometry of the design proposal in a lower dimensional skeleton. There are several skeletonization algorithms known. They originate in computer graphics, animation industry and CAD-modeling. Skeletons aim for mid-lines (curve skeleton) or more recently mid-surfaces (surface skeleton) [14], [28], [36]. The skeleton afterwards acts as reference for the generation of higher dimensional geometry (Fig. 3). This strategy is applied by Stangl and Wartzack [34], as well as Nana et al. [30], Cuillière et al. [11], Amroune and Cuillière [5] and Kresslein et al. [23] with contraction based curve skeletons. By extruding a defined cross-section along the reference curve, parametrically referenced 3D CAD-geometry can be created. The resulting polygonal line-segments are manually converted to b-spline curves in Stangl and Wartzack [34]. Similarly, Kresslein et al. [23] perform a change of previously segmented curve-skeleton-segments in b-splines, while Nana et al. [30] and Cuillière et al. [11] perform a normalization in straight line segments. Amroune et al. [5] use postprocessed, polygonal line segments and in particular focuse on the junction area inbetween. The software Materialise 3matic also provides the possibility to compute skeleton lines and assisting software tools for manual operation of surface based reconstruction [7]. Liu et al. [25] use curve skeletonization for smoothing the contour of a planar structure before this structure is approximated with cubic b-splines. Again based on curve skeleton, Denk et al. [13] propose a method by use of a homotopic thinning algorithm. Here, a distance transformation is applied to models, generated from volumetric pixels (voxels). This way, cross-section information can be computed. A similar procedure with a thinning algorithm is found in works by Yin et al. [41] and Alves and Siefkes [3]. Resulting curve skeletons are simplified by neighborhood relations of each single element and imported in the CAD environment as straight line wire model [3]. All together, the curve skeleton methods are partially automated approaches with manual intervention at critical steps. They are suited for beam-like structures. At junction points between skeleton lines or the referenced volume geometry they face difficulties in the correct combination of single cross sections. This issue is pointed at already in works of Subedi et al. [35], Cuillière et al. [11], Kresslein et al. [23] and Amroune et al. [5]. The difficulty in junction areas stems from the skeleton direction, which in these areas rarely fits to the actual geometry placement. Further, the identification of a cross-section in the area of junction is difficult. Contraction algorithms may even show skeleton parts outside of the input geometry. Especially non-beam-like structures, at which the length-to-width-ratio of a cross section tends to one side, are difficult, because they hardly can be abstracted by a one-dimensional line and deviations in topology are possible. If holes in the structure are represented topologically, they still can deviate geometrically, which makes reconstruction additionally difficult. Fig. 4 shows some of these difficulties at the curve skeleton computed by the contraction based mean curvature flow algorithm [37]. Exemplary used is the design proposal of a non-beam-like structure. The curve skeleton shows spurious branches and knots, where no knots would be expected intentionally. Further, it partially lies out of the bounds of the design proposal. A reconstruction strategy, in which cross-sections should be computed depending on the curve skeleton, inevitably faces problems especially in the area of these knots, as well as the varying direction in the skeleton.

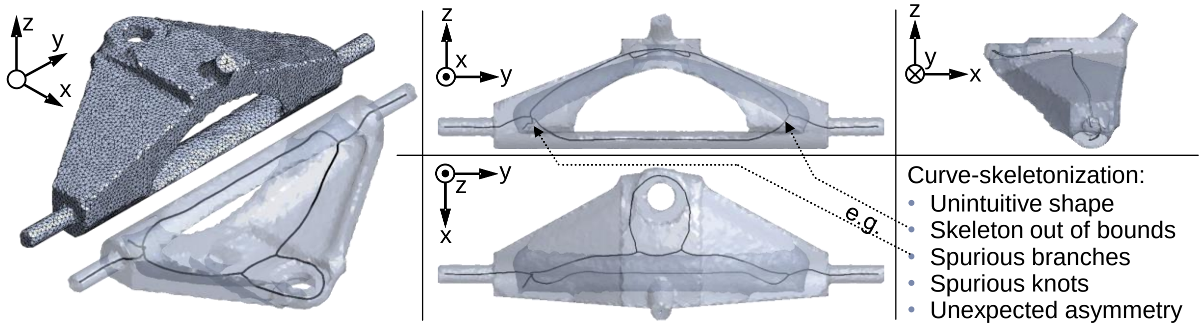

Figure 4: Typical characteristics of a curve skeleton in skeletonization of a non-beam-like structure.

As an alternative to curve skeletons a surface skeleton can be used. So Denk et al. [14] compute a surface skeleton, whose boundary curve is converted to a boundary line based control grid for subdivision-surfaces. This way, a reconstruction of non-beam-like geometry is possible, but parametrics are not incorporated and depending on the case the original shape may not be covered. Because there are several skeletonization strategies known, in the authors' previous work [28] meso-skeletons and the Medial Axis Transform were compared. After skeletonization as first step, possible reconstruction strategies were researched with the introduction of a decomposition structure [27]. The connection of animation industry's typical polygonal modeling and engineering's typical CAD-modeling contributes to the evolved decomposition in [29]. All aspects are explained in detail below.

3 METHOD FOR A NEW APPROACH TO COMPUTATIONAL TOPOLOGY RECONSTRUCTION

3.1 Overview

Geometry reconstruction in the focus of this work starts with the original TO-result exported as triangulated surface model. The following sections give a description on our computational reconstruction. We use the Medial Axis Transform for surface-skeletonization (section 3.2). Resulting data is processed to the decomposition structure (section 3.3). This is the basis for the geometry generation that implements parametric reconstruction through the skeleton's shape and Medial Axis geometry information. The Medial Axis originated information is the foundation for implemented high-level design features (section 3.4). The method has been implemented as a software tool. It works automatically, but offers optional manual editing of parametrics and features. The given design freedom and design exploration is specifically presented (section 4). Principal explanation of our method is given at a demonstrating cantilever for intuitive comprehensibility (section 3 to 4). Results for practical 3D-TO-models are investigated afterwards (section 5). These examples are given to also highlight the method's broad applicability.

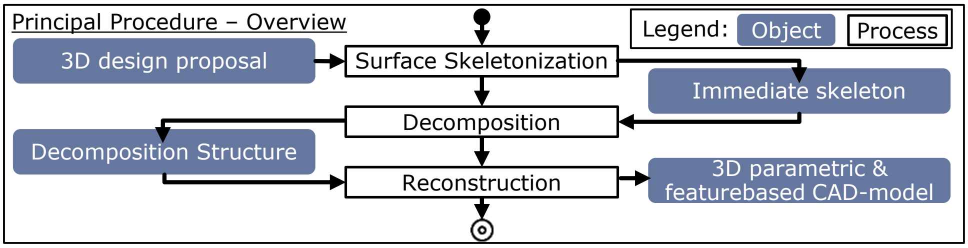

Figure 5: Principal procedure in the presented computational geometry reconstruction with the Medial Axis Transform.

3.2 A Different Way of Shape Description – Medial Axis Skeletonization

At first, the abstraction of topology optimization design proposals is carried out with surface skeletonization. For several reasons, we choose the Medial Axis Transform over contraction-based algorithms: it is principally computed parameter-free and automatically. It generates additional data on cross-section-information and works independently from geometrical shape for beam-like as well as non-beam-like structures. [28] The Medial Axis (Skeleton) originated as mathematical shape descriptor [8]. Contrary to the common Boundary Representation (B-Rep), it describes a shape alternatively by the set of centers of maximally inscribed balls [4]. This, together with the distance to the closest points on the input shape's boundary, adds up to the Medial Axis Transform (MAT). The MAT is the infinite set of the union of balls. It can be considered information-equivalent or dual to B-Rep [4]. Because the exact computation of the MAT is difficult, oftentimes a simplified, approximate version with a finite set of Medial Balls is computed [4]. Since TO's design proposal is represented by a discrete number of triangular facets, this also is the case for our method.

Voronoi diagrams are used for MAT computation of input sample points in our method. A voronoi diagram of a set of sample points separates space in convex polyhedral cells, such that within each cell the distance to the associated sample point is closest. Here, the euclidean distance metric is used. In Figure 6 the relevant data on voronoi cells consisting of voronoi vertices building the voronoi skeleton is visualized in 2D.

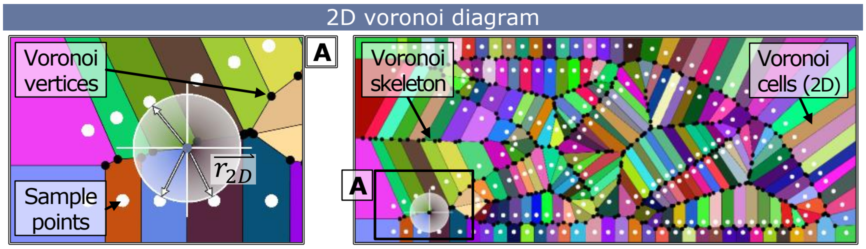

Figure 6: 2D Voronoi diagram of a point cloud with a maximal inscribed medial circle (left).

Voronoi vertices are the corner points of the Voronoi cells in $\mathbb{R}^2$ resp. in $\mathbb{R}^3$. They are mandatorily equally distanced from at least two nearest sample points. This property makes them important for the Medial Axis, which is the closure of the set of all vertices with more than one closest point on a shape's boundary. In 2D, the Voronoi skeleton is a *curve* skeleton, whereas in the general 3D case, it becomes *areal* (*surface* skeleton). In Figure 7 relevant data on a 3D-voronoi diagram is visualized.

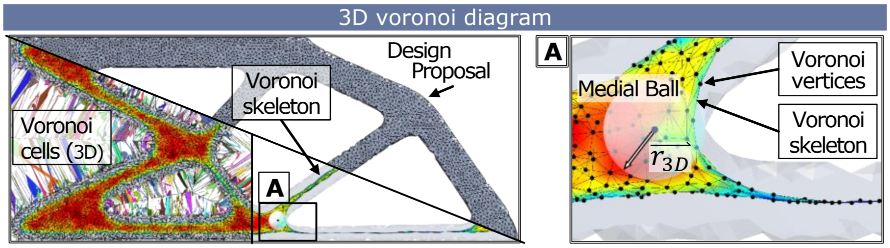

Figure 7: Optimized 3D cantilever with triangulated Medial Axis Skeleton and Medial Ball (right).

There are Voronoi vertices in- and outside of the sample points. Though the Voronoi vertices with their distance to at least two input points suit the definition of Medial Balls in 2D, the Voronoi vertices in 3D are not yet equivalent for Medial Axis computation. Again, they lie both inside and outside of the input shape. Second, amongst the in- and outliers respectively, only a subset of Voronoi vertices represents the Medial Axis. This subset is the so-called "poles" that corresponds to the two Voronoi vertices of a Voronoi cell most far away on either side of the input surface [4]. The outer poles belong to the outer Medial Axis, while the inner poles belong to the inner Medial Axis Skeleton. The poles' connectivity follows the sample points' connectivity. So in the more complicated, general 3D case, this Voronoi skeleton of inner poles is an approximation to the Medial Axis [33]. Onwards this is denoted as Medial Axis. The Medial Axis in Fig. 7 is colored with regard to the value of the Medial Balls' radii. For computation, the requirement of sufficiently dense input sample points has to be fulfilled [4]. In our approach this is assumed to always be the case, since the mesh of the design proposal can be subdivided arbitrarily fine. The design proposal's mesh is isotropically remeshed before skeletonization. For determination of interior and exterior we rely on the usually given surface normals. Resulting from the MAT-computation is a triangulated surface again. The Medial Axis Skeleton's mesh quality is very poor, with overlaying edges, redundant nodes and non-manifold geometry. Design proposal's significant geometry-elements are displayed qualitatively, not explicitly. For example, junction-edges are not represented by a single edge in the skeleton, but by several, jagged edge-segments. Informally speaking, the Medial Axis computation could be imagined with vacuum packing a volume. Then, the Medial Axis locates, where opposing surfaces meet. This effects in several surface segments stacked into each other, complicating the geometric data structure. In addition, the Medial Axis represents even the slightest unsteadiness in geometry, leading to large slivers in the skeletal form. Nevertheless, its definition follows the consistent scheme of maximally inscribed balls. The radii of the medial balls are additionally gathered information about local geometric thickness of the design proposal. The approach uses this geometry information in a later stage for the incorporation of parametrics and features.

For a cleaner Medial Axis, a smoothing is performed before and after the computation. Each vertex position is replaced by the average of its neighbors' positions. Smoothing before MAT computation is applied to the sample points in ten iterations. After MAT computation it is applied to the MAT skeleton in five iterations. Also, the resulting Medial Axis is simplified by merging relatively close vertices. This affects all neighbors within 25 % of the average edge length in the design proposal. The connectivity is updated accordingly. Those simplification steps reduce vertex count, but don't change either topology or geometry of the Medial Axis. They also do not provide manifoldness, nor remove all self-intersections. From this skeletonization resulting data, geometry reconstruction is not yet possible. The next step is therefore to purposefully process the information available up to this point into a decomposition structure.

3.3 Skeleton-Retopology

As preparation for the setup of a decomposition, from where reconstruction is possible, the skeletonization data is modified. For feasible reconstruction, no self-intersections must remain. Also, an important aspect is the ability of quads to be converted to T-Spline faces. While the skeleton at first in the process is triangular, it is converted to a quadrangular polygonal structure in the following under use of the graphics software Blender3D. In polygonal modeling this task is well known as *retopology*. It describes the generation of a new, pure quadrangular mesh ("quad mesh") from a finely discretized starting mesh. Retopology is a manual step. In our context, there are typically only few quad elements necessary to substitute the design proposal's Medial Axis. Via subdivision the resolution can be increased to any reasonable degree, later. Furthermore the quadrangular surface reduces vertex count. The data structure therefore requires less storage space. Bore holes etc. do not need to be represented in the quad mesh. They are incorporated as non-design geometry if they have already been in the design space. Otherwise, such features can be incorporated afterwards, because the final reconstruction result will be a CAD-model that suits further CAD-editing if necessary.

3.4 Parametric and Feature Based Computational Geometry Reconstruction

3.4.1 Non-design regions

Certain areas of the design space within TO have to be filled with material independent of the actual optimization, such as boundaries, fluid guidance, etc. Consequently, this passive area or non-design-area reappears in the final CAD-model in an unchanged form. This property is used for an automatic identification by comparing the design space with the design proposal. Though the passive area is geometrically untouched, it is nevertheless exported from TO as triangulated facets, too. Our algorithm splits the design space model in B-Rep entities, such as faces and curves by accessing the internal data structure of the step file in the CAD-kernel openCascade. Then, the triangulated facets are evaluated for their individual positions. If a face of a design space model is represented by facets to a specific level of its face area, the algorithm identifies that face as passive area. That way, a set of faces is highlighted as non-design geometry. At this point, the analytical face representation from the design space can already be used and does not have to be reconstructed. With the face representation itself, an eventual face type like planer or circular is known.

3.4.2 Lead structure

The main part of the optimized material distribution is reconstructed algorithm-wise under use of skeletonization thickness data. For this, the Medial Axis radii are mapped from the original skeleton mesh to the new quad mesh. This is done automatically with nearest neighbor search between mesh nodes from both sets. The radii are superimposed according to the nearest neighbor found (Fig. 8).

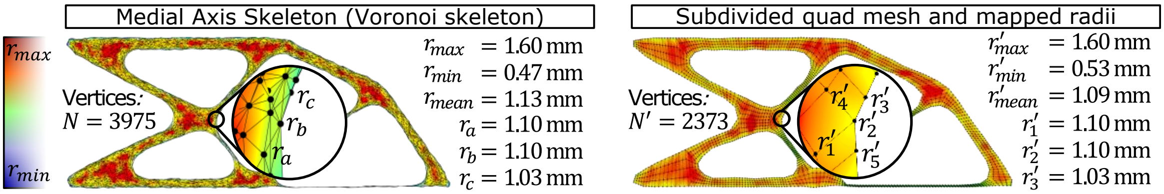

Figure 8: Mapping of Medial Axis radii to the quadrilateral mesh structure.

After the mapping step, the radii values are smoothed depending on the neighbors' radii. Especially if a small amount of quad skeleton vertices is used, this smoothing standardizes cross section variation in the geometry. However, if sticking with original values is the priority, the smoothing can of course also be disabled. The numerical amount of quad skeleton vertices determines the resolution of the MAT's radii within the geometry reconstruction. If more detailed distribution of vertices is desired, a subdivision can automatically be performed to any degree *before* the mapping step. This is the more important, the more varying cross-section values should be considered. If subdivision is performed *after* the mapping step, the newly created vertices will automatically inherit their weights from their respective predecessor vertices.

Based on the radii as thickness information and the quad skeleton as local information, the quad mesh is dilated. This is implemented as a basic construction feature for this approach (Fig. 9). Because the approach is automated as far as possible, per default the radii are considered as cross-section values. An advantage nevertheless is the possibility to freely edit these values. For example, the cross-section-thickness of selected parts can be set to an identical value by manipulation of the radii. This can be done with regard to manufacturing purposes or other conceivable options like even design optimization. Besides the dilation feature, another important feature concerns rim design. Because pruning the Medial Axis' spurious branches shrinks the skeleton, the specific dilation alone does not fully reconstruct the design proposal's volume. Again, this feature works with Medial Axis radii per default. It reconstructs the rim geometry in a semicircular shape (Fig. 9). Just like the dilation feature, the rim feature can be edited to free wishes. Instead of semicircular, a rectangular rim is implemented as another basic shape. Both shapes can be edited in individual, grouped, or general sets and by the change of parametric values. That means that closely specified parts of the rim, as well as global rim shape in general can be enlarged, minimized or otherwise edited.

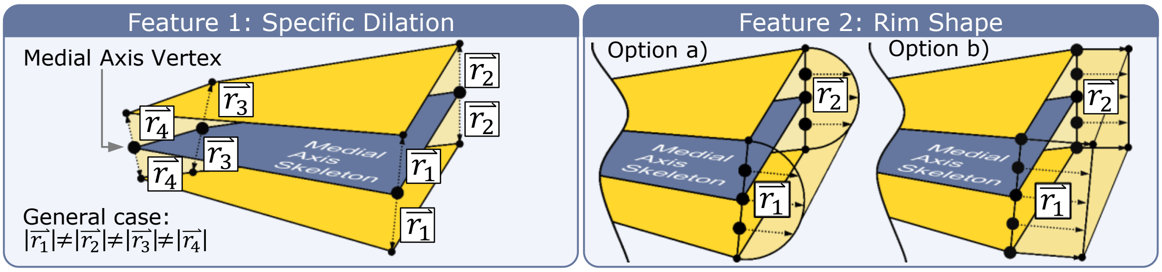

Figure 9: Features in the new approach for computational geometry reconstruction under consideration of Medial Axis incorporated parametrics.

Once the design is finalized, the geometry is exported in the wavefront-obj data format that preserves the quadrangular mesh structure. This in turn is imported in the CAD-system (here: Autodesk Fusion 360), where intermediate T-Spline conversion and subsequent conversion to analytic surfaces is performed. Parallel to the reconstructed geometry, the ideal geometry elements extracted by the non-design domain are imported in the CAD system. The final CAD-model is obtained by including the non-design domain in the model. Mostly this is done with Boolean operations. From then on, the geometry represents proper CAD-geometry and is ready for downstream applications.

4 DESIGN EXPLORATION: GEOMETRY AND TOPOLOGY EDITING WITHIN RECONSTRUCTION

Automation on the one side is necessary and beneficial for time and supportive aspects. Our approach can be used automatically without much effort. On the other side further potential is offered by optionally editing the reconstruction model in regard of many conceivable constraints. First, this is allowed through the Medial Axis Skeleton and second, through the Medial Axis radii. Our approach automatically uses the radii as basic thickness information per default (Fig. 10a). When new design requirements occur, special constraints must be considered or various designs should be explored, they can be edited directly within the reconstruction approach. Editing is possible both in the graphical user interface of Blender3D and by intervention in the program code. This can specify a single radius or it can concern several or all radii. Fig. 10 shows exemplary usage for increasing the struts overall wall thickness in z-direction with linear decrease along the y-axis (Fig. 10b). Also, independently from the increase in z-direction, the struts' diameter in the xy-plane is increased (Fig. 10b). Beyond geometry, topology can be edited within our approach, too. For example elements can be inserted or removed by manipulation of the quad mesh (Fig. 10c). The newly created vertices' radii are added in the loop, so geometry synthesis remains executable.

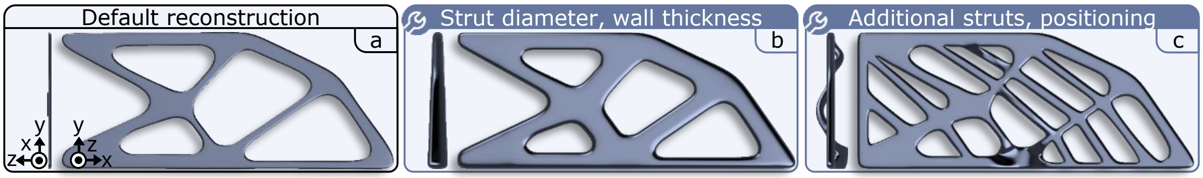

Figure 10: Editing options of geometry and topology within our approach (same demonstrator).

5 APPLICATION ON STRUCTURAL COMPONENTS AND MECHANICAL PROPERTIES OF THE RESULTS

The new reconstruction approach is tested with different demonstrators.

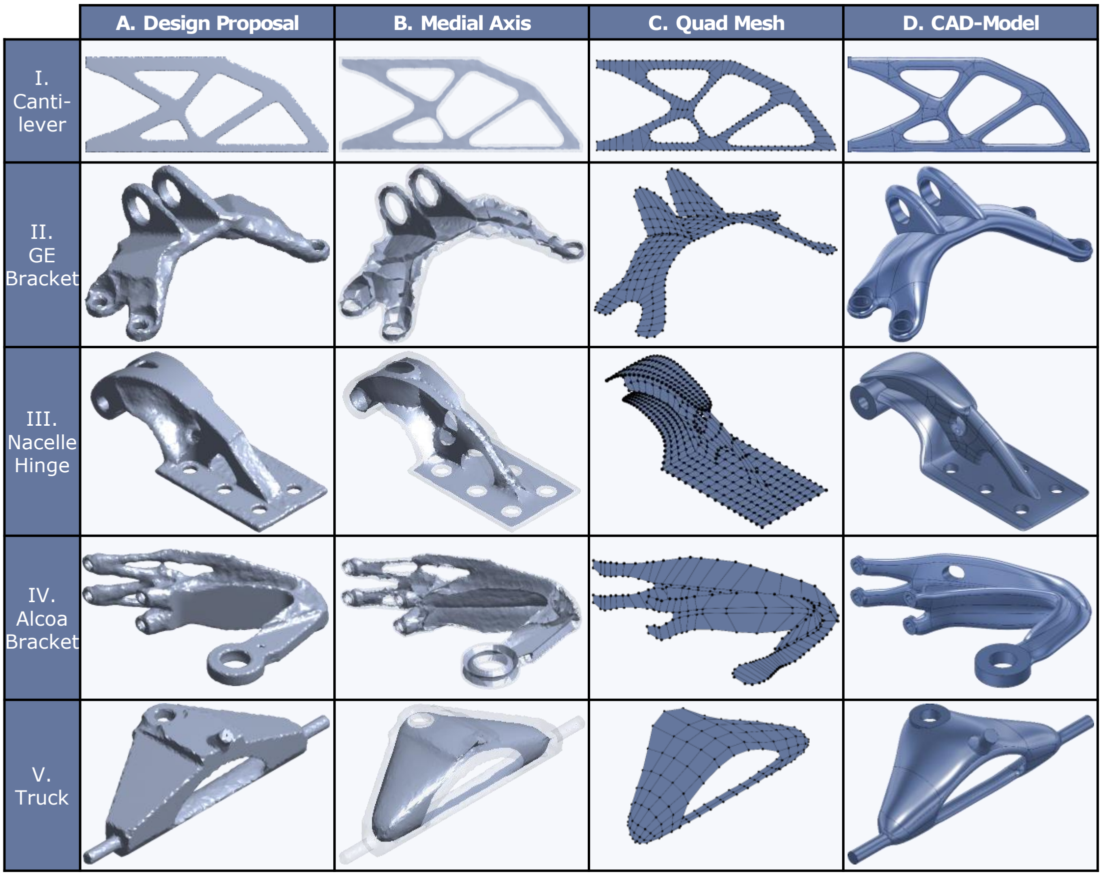

Figure 11: Design proposal, Medial Axis Skeleton, quad skeleton and resulting CAD-model.

In addition to a 3D cantilever (Fig. 11, I.), practical models of structural components are used. The GE Bracket (II.) [9], [15] and Alcoa Bracket (IV.) [1] come from public design challenges. The nacelle hinge (III.) was presented in an application study [39] and is part of previous work [29]. The truck (V.) is self-created with regard to a surface-like structure. Fig. 11 shows the design proposals (A.), the skeletonization step's resulting Medial Axis Skeletons (B.), the decomposition's quad meshes (C.) and the finally exported CAD-models (D.).

For this comparison the approach is applied with the possibilities described in the previous chapter and the intention to best represent the design proposal's material distribution. Specifically, for the model I. the rim feature thickness is increased by factor 2.5, specific dilation by 1.25. For II. the wall thickness is increased in the lateral areas of greatest expansion. The bolt lugs are leveled planar by simply editing the skeleton and their wall thickness is standardized to the value of 8.5 mm. In III. the wall thickness in the curved section is increased. Though design exploration such as generation of several CAD-models at once would be possible, other design goals or constraints are not considered. For the presented demonstrators in Fig. 11 structural analyses are performed in order to estimate the reconstruction quality and to validate the method (Fig. 12).

	I.Cantilever	II. GE Bracket		III. Nacelle Hinge		IV. Alcoa Bracket			V. Truck	
Characteristics of topology optimization setup										
Elements	7064	79,987		161,833		109,700			132,415	
Loadcases	1.	1. 3.	2. 4.	1.	2.	1.	2.	3.	1.	2.
$v_f^{objective}$	40 %	30 %		40 %		30 %			35 %	
Characteristics of resulting design proposal										
$v^{design\ proposal}$	22,087 mm³	140,100 mm³		191,060 mm³		32,547 mm³			32,292 mm³	
$v_f^{design\ proposal}$	41 %	30 %		42 %		30 %			36 %	
Elements	34,749	176,671		35,897		179,360			106,572	
Strain Energy Sum $c^{design\ proposal}$	1.533 mJ	3927 mJ 2719 mJ	5185 mJ 957 mJ	567 mJ	2075 mJ	5862 mJ	4194 mJ	3937 mJ	32,9 mJ	30,5 mJ
Maximum displacement	0.032 mm	0.34 mm 0.16 mm	0.42 mm 0.11 mm	0.18 mm	0.47 mm	1.65 mm	2.07 mm	1.56 mm	0.08 mm	0.13 mm
$k^{design\ proposal}$	0.0339 kJ·mm³	550 kJ·mm³ 381 kJ·mm³	726 kJ·mm³ 134 kJ·mm³	108 kJ·mm³	396 kJ·mm³	191 kJ·mm³	136 kJ·mm³	128 kJ·mm³	1.063 kJ·mm³	0.983 kJ·mm³
Characteristics of reconstructed CAD-model										
$v^{CAD-model}$	20,987 mm³	126,210 mm³		163,319 dm³		33,243 mm³			26,195 mm³	
$v_f^{CAD-model}$	39 %	27 %		36 %		30 %			30 %	
Elements	29,761	136,170		161,833		133,845			125,985	
Strain Energy Sum $c^{CAD-model}$	1.739 mJ	4342 mJ 2690 mJ	5946 mJ 758 mJ	538 mJ	2523 mJ	5444 mJ	3920 mJ	3718 mJ	49.2 mJ	31.0 mJ
Maximum displacement	0.037 mm	0.39 mm 0.16 mm	0.51 mm 0.09 mm	0.19 mm	0.60 Mm	1.50 mm	1.91 mm	1.46 mm	0.12 mm	0.14 mm
$k^{CAD-model}$	0.0365 kJ·mm³	548 kJ·mm³ 339 kJ·mm³	750 kJ·mm³ 96 kJ·mm³	88 kJ·mm³	412 kJ·mm³	181 kJ·mm³	130 kJ·mm³	124 kJ·mm³	1.29 kJ·mm³	0.81 kJ·mm³
v: volume v_f: volume fraction c: compliance k: comparison key figure, $k = c \cdot v_f$										

Figure 12: Simulation results of the five selected demonstrators.

In the initial TO and in the finite element analysis isotropic material is used throughout. The analyses are set static implicit with linear elastic material in all simulations. Depending on the model, there are one to four load cases applied. The load cases are identical in the respective optimization and the respective static structural simulation. Fixing and load application points are non-design-area and ensured to be positionally accurate in design proposal and reconstructed model. In each case the design proposal's simulation result is the reference for a comparison with the reconstructed model. This is based on a comparison key figure computed by multiplication of strain energy sum and volume (Fig. 12) [31]. This way, compliance is evaluated with respect to different volume fractions: the lower the key figure is, the better. Depending on the reconstructed model's performance the value is colored in green or orange in Fig. 12. Results show the reconstructed models to have lower stiffness in four of twelve cases. In the other eight cases, the reconstructed model even outperforms the design proposal. This is due to the fact, that exceedance of the initial design space for TO is not explicitly hindered until now.

6 DISCUSSION

The presented holistic approach to geometry reconstruction has the objectives of parametric and feature based reconstruction in an automatic way for non-beam-like geometry.

Parametrics & Features – Every design proposal in Fig. 11, A. is represented by a triangulated surface, whose information content is limited to an interconnected point cloud. However, the abstraction through Medial Axis Skeletonization provides the further geometric information of the radii of the maximal inscribed spheres, besides the Medial Axis Skeleton itself. Build on the Medial Axis Skeleton and the radii as distance measure, parametrics and features are implemented later. The Voronoi-computed Medial Axis Skeleton in every shown case first is a self-intersecting, non-manifold surface (Fig. 11, B.). In proceeding from the Medial Axis to the quad mesh (C.), there is still an interpretation by the user incorporated. This concerns superfluous, spurious branches in the Medial Axis that are unnecessary to represent in the quad mesh, because they reflect negligible shares of the design proposal. Since TO's non-design domain is processed in parallel, it therefore does not need to be considered in the quad mesh either. Thus, in Fig. 11 II.C to V.C. bore holes are not considered, which in turn simplifies the retopology step. The skeleton's geometry as well as the radii can be edited variable-based within the reconstruction itself. This way, the approach achieves to parameterize the typically freeform-shape of TO's design proposals. In the end, feasible CAD-files are generated, that could be edited again in CAD-environment. As the demonstrators (Fig. 11) show, the geometries represent the design proposals closely. The resulting good mechanical characteristics underline structural integrity. The mostly better performance of the reconstructed models over their design proposals show that the presented approach is capable of producing stiff and light models and that strict spatial constraining may limit structural performance. Outperforming the design proposals is at the cost of design space exceedance, which is caused by the intermediate processing steps of smoothing before and after skeletonization, retopology and design editing. Likewise, the strict adherence to the design space was no priority in these studies. Occurring exceedances are slight and could be prohibited by the active use of the method's featured editing options themselves. If not for strict adherence to the design space, editing otherwise may be used to adapt the geometry to practical requirements of product development and structural components. Manufacturing or other constraints and various design exploration are considerable.

Full automation – On the one hand, the interpretation in the retopology step (Fig. 11, B. to C.) counteracts full automation. On the other hand, it preserves flexibility to respond to different geometry and constraints as well as creativity. We found interpretation and creativity difficult to map in a fully automated *and* robust algorithm producing feasible results. Of course, further constraints for a guaranteed design space adherence could be implemented. For example, Boolean operation would be possible. In doing so, it must be taken into account, that load paths are not interrupted. Until now, this is a manner of interpretation, such as the Boolean incorporation of the non-design domain. Bypassing the geometry treatment of non-design geometry assures the exact geometric position of non-design area, which often holds load transfer points. Oftentimes a more refined combination of main geometry and non-design domain can be performed by manual interpretation. For these aspects, fully automation in this approach may not be the best solution in terms of feasibility of resulting models at this time. This also is the reason for the link between the two essential steps of geometry abstraction and geometry synthesis not to be automated yet. Here, interpretation still is necessary. Through the common retopology step this is rather quick to perform. Instead of 3D-geometry, only the 2D surface skeleton has to be considered. Nevertheless, because it assists and accelerates product development, automation is aimed for as far as possible. The two essential steps themselves, geometry abstraction and the otherwise labor-intensive geometry synthesis of the lead structure, are fully automated. This means, the skeletonization step in the first place, and the lead structure's geometry generation are automatically processed. The approach therefore drastically reduces the time necessary to generate feasible CAD-models.

Non-beam-like geometry: As shown with the five demonstrators (Fig. 11) the method provides feasible results for academic and real life applications. Demonstrator I. shows application at a beam-like structure. The approach also works with beam-like geometry for the reason that a beam still can be represented by a narrow face in the decomposition structure. The other demonstrators II. to V. represent the particularly focused non-beam-like geometry, for which the presented computational approach provides feasible results by using the Medial Axis. Resulting models are able to be used in product development's downstream applications like structural simulations.

7 CONCLUSION AND PERSPECTIVES

Automatically receiving feature based CAD-models from TO holds large potential for product development. It contributes to an even broader use of TO and its integration in the development process. Benefits in reduced development time and lightweight design are provided simultaneously. A computational instead of an experience-dependent, manual design approach makes geometry reconstruction more independent of individual influences. Fully automated geometry reconstruction for general, geometrically varying TO results remains a challenge. Research on fully automated retopology will be interesting for maximizing the degree of automation. Our approach provides broad applicability from beam-like to especially non-beam-like structures. It yields editable parametrics and features, which in turn offers design freedom. This is planned to be used for parameter optimization in our future work. Starting from the TO's stiffness optimization this could be done with regard to structural strength. For future work we also intend to develop the approach to consider further constraints like manufacturing and product aesthetics.

8 ACKNOWLEDGEMENT

The authors thank Dr.-Ing. H. Völkl and Dr.-Ing. M. Denk whose comments helped improve and clarify this contribution. The presented research work is funded by the Deutsche Forschungsgemeinschaft (DFG, German Research Foundation) – WA 2913/36-1 with the title „TopoRestruct – Rückführung fertigungs-, beanspruchungs- und funktionsgerechter Konstruktionsgeometrie aus Ergebnissen der Topologieoptimierung in den Produktentwicklungsprozess". The authors thank the German Research Foundation for the financial support.

Johannes Mayer, http://orcid.org/0000-0002-1280-217X
Sandro Wartzack, https://orcid.org/0000-0002-0244-5033

REFERENCES

[1] Alcoa Fastening Systems & Rings: Airplane Bearing Bracket Challenge (2015), [Online], available at: https://grabcad.com/challenges/airplane-bearing-bracket-challenge. [Last accessed Nov 2, 2022].

[2] Allen, G.: nTopology Modeling Technology, Whitepaper, 2019. Available at: https://ntopology.com/blog/implicit-modeling-for-mechanical-design/. [Last accessed Nov 2, 2022].

[3] Alves, C. G.; Siefkes, T.: Automatische Erstellung von Drahtgittermodellen aus Topologieoptimierungen, In: Stuttgarter Symposium für Produktentwicklung SSP 2021, Stuttgart, Germany, 2021. https://doi.org/10.18419/opus-11478
[4] Amenta, N.; Choi, S.; Kolluri, R. K.: The Power Crust, Unions of Balls, and the Medial Axis Transform, International Journal of Computational Geometry, Theory and Applications, 19(2-3), 2001, 127-153. https://doi.org/10.1016/S0925-7721(01)00017-7
[5] Amroune, A.; Cuillière, J.-C.: Automated Lofting-Based Reconstruction of CAD-Models from 3D Topology Optimization Results, Computer-Aided Design, 145(1), 2022, Article 103183. https://doi.org/10.1016/j.cad.2021.103183
[6] Bendsøe, M. P.; Sigmund, O.: Topology Optimization: Theory, Methods and Applications, Springer, Berlin, 2004.
[7] Blanc, C.: 3-matic STL 9.0. Von der Topologieoptimierung zum gedruckten Bauteil, Materialise beschreitet neue Wege, In: 11th Coachulting Forum, Wernau, Germany, 2015.
[8] Blum, H.: A Transformation for Extracting New Descriptors of Shape, Models for the Perception of Speech and Visual Form, MIT Press, 362-380.
[9] Carter, W.; Erno, D.; Abbot, D.; Bruck, C.; Wilson G.; Wolfe, J.B.; Finkhousen, D.M.; Tepper, A.; Stevens, R.G.: The GE Aircraft Engine Bracket Challenge: An Experiment in Crowdsourcing for Mechanical Design Concepts, In: 2014 International Solid Freeform Fabrication Symposium, Austin, Texas, 2014, 1402-1411. https://repositories.lib.utexas.edu/handle/2152/89299
[10] Cuillière, J.-C.; Francois, V.; Drouet, J.-M.: Towards the Integration of Topology Optimization into the CAD Process, Computer Aided Design and Applications, 11(2), 2013, 120-140. https://doi.org/10.1080/16864360.2014.846067
[11] Cuillière, J.-C., François, V.; Nana, A.: Automatic construction of structural CAD models from 3D topology optimization, Computer Aided Design and Applications, 15(1), 2017, 107–121. https://doi.org/10.1080/16864360.2017.1353726
[12] Delame, T.; Kustra, J.; Telea, A.: Structuring 3D Medial Skeletons: A Comparative Study, In: Hullin, M.; Stamminger, M.; Weinkauf, T. (eds.): Symposium on Vision, Modeling and Visualization, Eurographics Association, Bayreuth, Germany, 2016. ISBN 978-3-03868-025-3; https://www.doi.org/10.2312/vmv.20161336
[13] Denk, M.; Rother, K.; Paetzold, K.: Fully Automated Subdivision Surface Parametrization for Topology Optimized Structures and Frame Structures using Euclidean Distance Transformation and Homotopic Thinning, In: Proceedings of the Munich Symposium on Lightweight Design 2020, 2020. https://doi.org/10.1007/978-3-662-63143-0_2
[14] Denk, M.; Rother, K.; Paetzold, K.: Subdivision Surface mid-surface reconstruction of topology optimization results and thin-walled shapes using surface skeletons, In: International Conference on Engineering Design, ICED21, Gothenburg, Sweden, 2021. https://doi.org/10.1017/pds.2021.538
[15] GrabCAD: GE Jet Engine Bracket Challenge, 2013. [Online], available at: https://grabcad.com/challenges/ge-jet-engine-bracket-challenge. [Last accessed Nov 2, 2022].
[16] Harzheim, L.: Strukturoptimierung: Grundlagen und Anwendungen, Europa-Lehrmittel, Haan-Gruiten, 2014. ISBN 978-3-8085-5882-9.
[17] Hessel, C.: Integration der Topologieoptimierung in den CAD-gestützten Entwicklungsprozess, Ph.D. Thesis, RWTH Aachen, Shaker, Aachen, 2003. https://publications.rwth-aachen.de/record/63461
[18] Hsu, M.-H.; Hsu, Y.-L.: Interpreting three-dimensional structural topology optimization results, Computers & Structures, 83(4), 2005, 327–337. https://doi.org/10.1016/j.compstruc.2004.09.005
[19] Hsu, Y.-L.; Hsu, M.-S.; Chen, C.-T.: Interpreting results from topology optimization using density contours, Computers & Structures, 79(10), 2001, 1049-1058. https://doi.org/10.1016/S0045-7949(00)00194-2
[20] Joshi, S.; Medina, J. C.; Menhorn, F.; Reiz, S.; Rüth, B.; Wannerberg, E.; Yurova, A.: CAD-integrated Topology Optimization, Bavarian Graduate School of Computational Engineering

project report, 2016. published online, https://www5.in.tum.de/pub/bgceproject2016report.pdf
[21] Kaloudis, A.; Poulias, A.: Creation of 3D geometry from topology optimization results, for thin-walled and casted parts, In: 13th European LS-DYNA Conference 2021, Ulm, Germany.
[22] Koguchi, A; Kikuchi, N.: A surface reconstruction algorithm for topology optimization, Engineering with Computers, 22(1), 2006, 1-10. https://doi.org/10.1007/s00366-006-0023-0
[23] Kresslein, J., Haghighi, P.; Park, J.; Ramnath, S.; Sutradhar, A.; Shah, J. J.: Automated cross-sectional shape recovery of 3D branching structures from point cloud, Journal of Computational Design and Engineering, 5(3), 2018, 368–378. https://doi.org/10.1016/j.jcde.2017.11.010
[24] Larsen, S.; Jensen, G.: Converting Topology Optimization Results into Parametric CAD Models, Computer Aided Design and Applications, 6(3), 2009, 407–418. https://doi.org/10.3722/cadaps.2009.407-418
[25] Liu, S.; Li, Q.; Liu, J.; Chen, W.; Zhang, Y.: A realization method for transforming a topology optimization design into additive manufacturing structures, Engineering, 4(2), 2018, 277-285 https://doi.org/10.1016/j.eng.2017.09.002
[26] Louhichi, B.; BenAmara, A.; François V.; Romdhane, L.: Automatic generation of CAD model based on CAE results, 2008. Published online, https://www.researchgate.net/publication/250750704_Automatic_generation_of_CAD_model_based_on_CAE_results
[27] Mayer, J.; Wartzack, S.: A concept towards automated reconstruction of topology optimized structures using medial axis skeletons, In: Proceedings of the Munich Symposium on Lightweight Design 2020, Munich, 2021. https://doi.org/10.1007/978-3-662-63143-0_3
[28] Mayer, J.; Wartzack, S.: Investigation of surface skeletonization methods for reconstruction of topology optimized structures, In: Proceedings of the 31st Symposium Design for X, DFX 2020. https://doi.org/10.35199/dfx2020.12
[29] Mayer, J.; Völkl H.; Wartzack S.: Feature-Based Reconstruction of Non-Beam-Like Topology Optimization Design Proposals in Boundary-Representation, In: Proceedings of the 33rd Symposium Design for X, DFX2022. https://doi.org/10.35199/dfx2022.21
[30] Nana, A.; Cuillière, J.-C.; Francois, V.: Automatic reconstruction of beam structures from 3D topology optimization results, Computers & Structures, 189(1), 2017, 62-82. https://doi.org/10.1016/j.compstruc.2017.04.018
[31] Rozvany, G.: A critical review of established methods of structural topology optimization, Structural and Multidisciplinary Optimization, 37(3), 2009, 217-237. https://doi.org/10.1007/s00158-007-0217-0
[32] Schumacher, A.: Optimierung mechanischer Strukturen - Grundlagen und industrielle Anwendungen, Springer, Berlin, 2013. ISBN 978-3-642-34700-9
[33] Siddiqi, K.; Pizer, S. M.: Medial Representations. Mathematics, Algorithms and Applications, Springer, 2008. ISBN 978-1-4020-8657-1.
[34] Stangl, T.; Wartzack S.: Feature based interpretation and reconstruction of structural topology optimization results, In: Proceedings of the 20th International Conference on Engineering Design (ICED15), 2015, Milan, Italy.
[35] Subedi, S.; Verma, C. S.; Suresh, K.: A review of methods for the geometric post-processing of topology optimized models, Computing and Information Science in Engineering, 20(6), 2018. https://doi.org/10.1115/1.4047429
[36] Tagliasacchi, A.; Delame, T.; Spagnuolo, M.; Amenta, N.; Telea, A.: 3D Skeletons: A State-of-the-Art Report, Computer Graphics Forum, 35(2), 2016. https://doi.org/10.1111/cgf.12865
[37] Tagliasacchi, A.; Alhashim, I.; Olson, M.; Zhang, H.: Mean Curvature Skeletons, Eurographics Symposium on Geometry Processing 2012, 31(5), 2012, 1735-1744. https://doi.org/10.1111/j.1467-8659.2012.03178.x
[38] Tang, P.-S.; Chang, K.-H: Integration of topology and shape optimization for design of structural components, Structural and Multidisciplinary Optimization, 22(1), 2001, 65-82. https://doi.org/10.1007/PL00013282

[39] Tomlin, M.; Meyer, J.: Topology Optimization of an Additive Layer Manufactured (ALM) Aerospace Part, In: Proceedings of the 7th Altair CAE Technology Conference 2011, 1-9.
[40] Yi, G.; Kim, N. H.: Identifying boundaries of topology optimization results using basic parametric features, Structural and Multidisciplinary Optimization, 55(5), 2017, 1641-1654. https://doi.org/10.1007/s00158-016-1597-9
[41] Yin, G.; Xiao, X.; Cirak, F.: Topologically robust CAD model generation for structural optimisation, Computer Methods in Applied Mechanics and Engineering, 369(1), 2020. https://doi.org/10.1016/j.cma.2020.113102
[42] Zaharinov, V.: CAD reconstruction after topology optimization, an approach with sections, published online: http://e-university.tu-sofia.bg/e-publ/files/2843_Doklad_Zaharinov_Sliven_2017Red.pdf